


RESEARCH ARTICLE

Feasible speeds for two optimal periodic walking gaits of a planar biped robot

Mathieu Hobon¹, Víctor De-León-Gómez², Gabriel Abba¹, Yannick Aoustin^{2*}  and Christine Chevallereau²

¹Laboratoire de Conception Fabrication Commande, EA 4495, Arts et Métiers ParisTech, Université de Lorraine, 4 rue Augustin Fresnel, 57078 Metz Cedex 3, France and ²Laboratoire des Sciences du Numérique, de Nantes, UMR 6004, CNRS, École Centrale de Nantes, Université de Nantes, 1, rue de la Noë, BP 92101, 44321 Nantes, France

*Corresponding author. Email: Yannick.Aoustin@univ-nantes.fr

Received: 19 March 2020; **Revised:** 3 May 2021; **Accepted:** 3 May 2021; **First published online:** 4 June 2021

Keywords: Walking gait, Finite-time double, Impact with foot flat, Toe impact, Heel impact

Abstract

The purpose is to define the range of feasible speeds for two walking motions for a particular planar biped robot, which differ in the definition of their finite-time double support phases. For each speed, these two walking motions are numerically obtained by using a parametric optimization algorithm, regarding a sthenic criterion. Results allow us to define the range of allowable speeds for each walking. One result is that the first gait is less consuming in energy for moderate to fast velocity with respect to the second one, while the second gait is more efficient for low walking velocity.

1. Introduction

This paper explores the range of feasible speeds for a planar biped that adopts two walking motions, which differ in the definition of their finite-time double support phases. The choice here of a planar biped is due to the fact that for human's walking gait, the main movements are executed in the sagittal plane, see refs. [1, 2]. Frontal plane movements mainly serve to keep human laterally balanced. The pelvis rotation has an important effect to limit the necessary energy to move the swing leg [3]. However, our purpose being to study the energy effect of two finite-time support phases, we assume that the results are little influenced by the pelvis rotation for the two gaits. The human walking is composed of single support phases and double support phases. For one step, the duration of a double support phase represents almost 24% of the time step [4]. Several papers are devoted to a borderline case where the step of walking is composed of a single support phase and an instantaneous double support [5]. For example, the relatively human-inspired ones, which have been tested with the biped robots *Amber* [6] and *Rabbit* [7] or the walking motions defined through the linear inverted pendulum [8] or ref. [9], among others.

However, for a biped robot, the contribution of the finite-time double support phase is important to change the velocity rate of the walking, to increase the domain of stability in order to reject some disturbance occurring in single support, see refs. [10], and [11] where planar bipeds with pointed feet are considered. Inserting a finite-time double support phase in a gait of a biped with feet implies to deal with the behavior of the foot and the over actuation of the locomotor system, since a closed chain is formed by the locomotor system and the ground. There is a actuation redundancy leading to an infinite number of solutions for joint torques and the ground reaction wrench. Ju and Mansour, [12] proposed a foot model with a curved planter surface to design a finite-time double support phase for the motion of a biped in sagittal plane. Sharma and Stein, [13] incorporate the finite-time double support phases and single support phases in walking of a biped with point feet to minimize muscle activation and arm

reaction forces generated from the walker. The dynamics-based optimization of sagittal gait cycles of a seven-link planar biped with feet by using the Pontryagin maximum principle is considered in ref. [14]. In there, one step is composed of a fully actuated single support phase and a finite-time double support phase and the velocity of the swing foot at the landing on the ground is zero. Six periodic gaits are presented in ref. [15]. The simplest periodic gait is composed of successive single support phases with a flat foot contact on the ground, and the stance foot does not rotate. The support phases are separated by instantaneous double support. The most complex periodic motion is composed of single support phases and finite-time double support. For the finite-time double support phases, the front foot rotates around its heel and the rear foot rotates around its toe. For this walking, with a finite-time double support phase there is no impact of the swing foot landing on the ground, as well as for the walking gait defined in ref. [10] for a biped with point foot and in ref. [16] where an impactless walking gait is carried out with single support phases and finite-time double support phases for a seven-link planar biped with feet. Nevertheless, it has been shown that the energy cost for the walking gait is smaller when the single support phases are ended with impacts than when the velocity of the swing foot at the landing is null [15]. An original design is proposed for the knee joints of a planar biped robot, based on a four-bar linkage. A comparison of the performances with respect to a sthenic criterion is proposed between a biped equipped with four-bar knees and the other with revolute joints for walking reference trajectories composed of single phases, impact, and finite-time double support phases with rotation of both feet [17]. The numerical results show that the performances with a four-bar linkage are worst for the smaller velocities and better for the higher velocities. Tan et al. [18] proposed a finite-time double support phase that begins when the swing foot strikes the ground and finishes with the support foot toe-off. The inverse dynamic model is used to optimize a walking gait with the objective that the trunk remains upright. The criterion is based on the altitude of the center of mass with respect to a reference. Simulation results show that a two-level control strategy for simultaneous gait generation and stable control of planar walking of the ATRIAS biped can reject initial condition disturbances, while generating stable and steady walking motion [19].

Despite all these interesting studies on walking motions with finite-time double support phases, there is a lack of knowledge about the role of the feet during the finite-time double support phase regarding on the speed of the biped robot. Several questions on this issue are still open such as:

- Can one foot stay on the ground with a flat foot contact after its landing while the other rotates?
- Can both feet rotate simultaneously after the landing of the swing foot on its heel?
- What are the feasible speeds for walking with finite-time double support phase? Feasible speed means, here, speed that satisfies the limits of the actuator and the unilateral constraints of the biped robot with the ground.
- What is the best strategy at impact to satisfy the unilateral constraints on both feet for a feasible speed?

The goal of this paper is to see if we can draw on anthropomorphic features to improve the walking of bipedal robots with rigid feet. Of course to design a human-like walking, there are many other interesting questions such as a foot-roll design, [20] or the rotation of the foot during the single stance phase [15]. But we want to focus our attention on the effect of finite-time double support phases for walking. In particular, the goal is to give a response to the four previous research questions for a set of periodic walking motions in the sagittal plane, which are composed of impacts, single support phases, and finite-time double support phases. The ground and the biped limbs are assumed rigid. These gaits are defined with a parametric optimization by using a sthenic criterion and with nonlinear constraints. Even if for human there are movements of bodies that take place in the frontal plane, we limit our numerical studies in the sagittal plane because the magnitude of movements are much larger. As a consequence, the results about the energy consumption that are obtained in the sagittal plane are usually confirmed by a study in the 3D space, see, for example, ref. [17]. The planar biped model is defined with the physical parameters of the experimental biped *Hydroid* [21]. Its inertial parameters are close to those of human. The step of the first gait is composed of a single support phase, with support on flat foot, a flat-footed impact on the

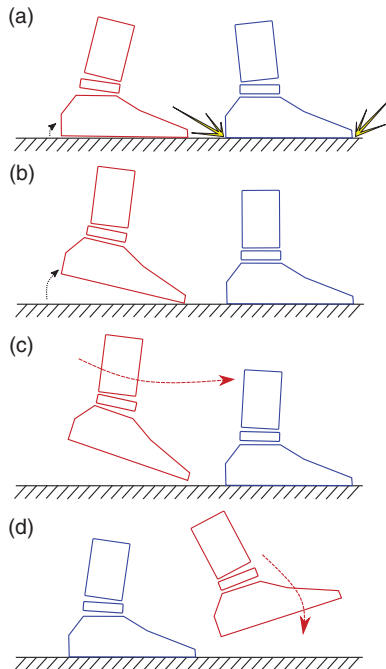


Figure 1. Walking motion 1. (a) End of the SS beginning of the DS. (b) DS. (c) End of the DS. (d) SS.

ground for the swing leg, and a finite-time double support phase, where the rear foot rotates around its toe and the front foot is kept flat on the ground. With this first walking motion, it is possible to answer “Yes” to the first question. The second walking motion design is similar to the first one, except that the single support is ended by a heel impact and during the finite-time double support phase, the rear foot rotates on its toe and the forward foot rotates on its heel. The finite-time double support of this gait is ended with a toe impact on the ground of the forward foot. With this second walking motion, it is possible to answer “Yes” to the second question. According to the experimental studies of Winter [4], this second walking motion is closer to the human walking motion than the first one. Studying these two walking motions, for various speed, will allow to answer the third and fourth questions. The algorithm for defining optimal walking gait has been carefully studied and programmed to converge to physically feasible solutions. When convergence was not achieved, it means that the bipedal robot could not achieve the walking gait with the target speed.

This paper is outlined as follows. Section 2 gathers the definition of the two walking motions. Section 3 presents the biped modeling for each phase of the walking motions. Section 4 deals with the trajectory planning. In Section 5, numerical results of the criterion evaluation as a function of the bipedal robot speed are presented. Finally, Section 6 offers our conclusion and proposes several perspectives.

2. Studied gaits

In the following, two types of walking motions are studied. A lot of articles are devoted to the definition of walking speeds with single support phases, instantaneous double supports [22], or with single support phases, finite-time double support phases but without impact, [16]. In order to offer the reader a simple and rigorous presentation, two walking more anthropomorphic motions with phases of simple support and finite-time double support and impact will be compared.

- Gait 1: The periodic motion is composed of single support and finite-time double support phases. At the end of the single support phase, see Fig. 1(a), there is a flat-footed impact on the ground. In double

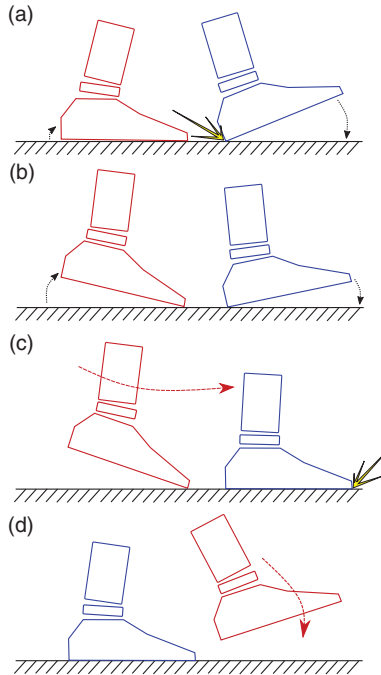


Figure 2. Walking gait 2. (a) End of the SS/beginning of the DS. (b) DS. (c) End of the DS. (d) SS.

support phase, the rear foot (foot 2) rotates on its toe, the other is flat on the ground, see Fig. 1(b). On Fig. 1(c), the finite-time double support is ended when the rear foot (foot 2) takes off the ground with the toe, the other foot stays flat on the ground. The single support takes place, see Fig. 1(d).

- Gait 2: The periodic motion is composed of single support and finite-time double support phases. At the end of the single support phase, see Fig. 2(a), the impacting foot (now foot 1) touches the ground with its heel. The rear foot (foot 2) keeps contact with the ground through its toe. In double support phase both feet rotate, see Fig. 2(b). The finite-time double support ends when the front foot (foot 1) impacts the ground with its toe and the rear foot (foot 2) takes off as shown in Fig. 2(c). Then the single support takes place, see Fig. 2(d).

The gait 1 maximizes the walking stability since the support area in finite-time double support is larger than the one of the gait 2. The gait 2 allows larger walking velocity than gait 1 since the distance between foot can be increased while respecting the joint limits.

3. The biped modeling

3.1. The biped

Let us consider a seven-link planar biped robot with physical parameters obtained from those of the 3D experimental biped *Hydroid* [21] and ref. [23]. A photograph of the locomotor system of *Hydroid* is shown in Fig. 3. The inertial parameters of *Hydroid* are inspired from the Hanavan model [24]. The considered planar biped is shown in Fig. 4. Table I gathers its physical parameters. The parameters s_i , $i = 1, \dots, 5$ define the position of the center of mass of the limbs and the trunk with respect to the hip and knee joints. The parameters l_f and L_f are the distances from the projection of the joint ankle on the foot sole with the heel and the toe, respectively. H_f is the distance between the ankle joint and the sole. S_{px} and S_{py} are the coordinates of the center of mass G_f of the foot with respect to the ankle joint. The lengths of the shins, thighs, and the trunk are, respectively, l_1 , l_2 , and l_t .



Figure 3. Photography of the locomotor system of Hydrorobot.

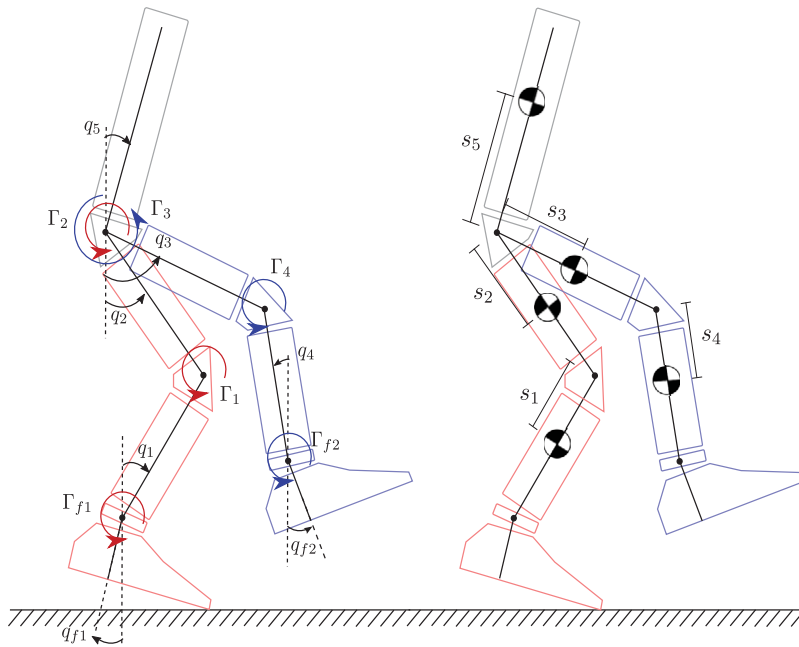


Figure 4. Schematic of the planar biped robot. Absolute angular variables and joint torques (the angular variables are counted positive counterclockwise).

3.2. Dynamic modeling: General case

Let us introduce the generalized vector \mathbf{q} for the description of the considered biped as follows¹:

$$\mathbf{q} = [q_{f1}, q_{f2}, q_1, q_2, q_3, q_4, q_5, x, y]^T.$$

The generalized variables x and y are the Cartesian coordinates of the hip joint. The other generalized variables are shown in Fig. 4. The vector \mathbf{q} is chosen with nine components including x and y in order

Table I. Physical parameters of the biped robot.

	Mass (kg)	Length (m)	Moment of inertia (kg.m ²)	Center of mass (m)
Foot	$m_f = 0.7$	$L_f = 0.21$ $l_f = 0.07$ $H_f = 0.07$	0.002	$s_{fx} = 0.01$ $s_{fy} = 0.03$
Shin	2.2	$l_1 = 0.4$	0.03	$s_1 = s_4 = 0.17$
Thigh	5.0	$l_2 = 0.4$	0.07	$s_2 = s_3 = 0.17$
Trunk	29.0	$l_t = 0.4$	0.8	$s_5 = 0.2$

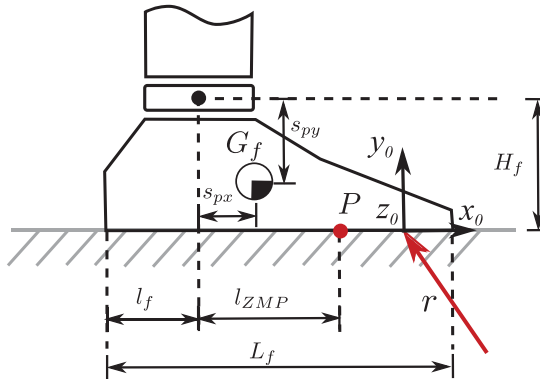


Figure 5. Details of the foot.

to be able to define a dynamic model that explicitly takes into account the unilateral constraints with the ground. For the studied walking motions, the contact with the ground of the biped can be with the whole sole, the heel, or the toe, see Figs. 1 and 2.

For any type of contact of the feet with the ground, the dimension of the robot given in Figs. 4 and 5 allows to write the condition to ensure a rigid contact between the feet and the ground based on geometric relation. Here, no slipping of the stance foot is assumed. Thus, the hypothesis of rigid contact implies zero velocity and zero acceleration of the foot relative to the ground.

By considering the virtual work principle, the matrix \mathbf{J}_i^T that allows to take into account the ground reaction $\mathbf{r}_i = [r_{ix}, r_{iy}, \mathcal{M}_i]^T$ in the dynamic model. This vector \mathbf{r}_i , defined in a frame (x_0, y_0, z_0) , see Fig. 5, represents the wrench corresponding to the reaction force and moment from the ground acting on foot i . If only one punctual contact between foot i and the ground is considered, the component of moment in \mathbf{r}_i (for a frame attached to the foot) is zero, that is $\mathbf{r}_i = [r_{ix}, r_{iy}]^T$.

Thus, the dynamic model of the biped robot is expressed as

$$\mathbf{D}(\mathbf{q})\ddot{\mathbf{q}} + \mathbf{N}(\mathbf{q}, \dot{\mathbf{q}}) + \mathbf{Q}(\mathbf{q}) = \mathbf{B}\boldsymbol{\Gamma} + \mathbf{J}_1^T(\mathbf{q})\mathbf{r}_1 + \mathbf{J}_2^T(\mathbf{q})\mathbf{r}_2, \tag{1}$$

with the constraint equations

$$\mathbf{J}_i(\mathbf{q})\ddot{\mathbf{q}} + \dot{\mathbf{J}}_i(\mathbf{q}, \dot{\mathbf{q}})\dot{\mathbf{q}} = 0 \quad \text{for } i = 1 \text{ to } 2. \tag{2}$$

Here, $\mathbf{D} \in \mathbb{R}^{9 \times 9}$ is the symmetric positive inertia matrix of the biped. Vector $\mathbf{N} \in \mathbb{R}^{9 \times 1}$ represents the centrifugal and Coriolis effects, and $\mathbf{Q} \in \mathbb{R}^{9 \times 1}$ is the effect of gravity vector. $\mathbf{B} \in \mathbb{R}^{9 \times 6}$ is a constant input mapping matrix composed of 1 and 0. $\boldsymbol{\Gamma} \in \mathbb{R}^{6 \times 1}$ is the vector of applied joint torques. \mathbf{J}_1^T and \mathbf{J}_2^T are the 9×2 (or 9×3 with a flat foot contact) transposed Jacobian matrices converting the ground

reaction wrench at feet 1 and 2 into torques applied at joints by considering a rigid contact. For the rigid contact of the foot 1 with the ground, the corresponding equations, in position, velocity, and acceleration are introduced in Appendix. In this appendix, Eqs. (A2) and (A4) describe a contact with the heel, and the Jacobian matrix, denoted in this case $J_1 = J_{h1}$ is given in Eq. (A3). Equations (A6) and (A8) describe a contact with the toe, and the Jacobian matrix, denoted in this case $J_1 = J_{t1}$ is given in Eq. (A7). Equations (A10) and (A12) are written for a foot contact flat on the ground with no take-off and no slipping of the whole sole, and the Jacobian matrix denoted in this case $J_1 = J_{f1}$ is given in Eq. (A11).

Equations (1) and (2) allow to describe any contact of the feet with the ground. These equations are usual in literature, however the case of finite-time double support is not often considered in detail. In this paper, an analysis of this phase is carried out in Section 4.

3.3. Impact model

In biped walking, an impact usually occurs when the swing foot touches the ground. For gait 2, an impact may also occur when the rear leg toe touches the ground. Let T be the instant of the impact. An absolutely inelastic impact is assumed, so that the foot does not slip. Given these conditions, the ground reactions at the instant of an impact can be considered as impulsive forces and defined by Dirac delta functions. Impact equations can be obtained through the integration of the equation of motion (1) for the infinitesimal time from T^- to T^+ . The vector of actuated torques and the Coriolis and gravity vectors have finite values. Thus, they do not affect the impact equations. Consequently the impact equations can be written in the following matrix form:

$$D(q(T))(\dot{q}^+ - \dot{q}^-) = J_{f1}^T(q(T))i_1 + J_{t2}^T(q(T))i_2. \tag{3}$$

Here, $q(T)$ denotes the generalized coordinates of the biped at instant $t = T$, (these generalized coordinates does not change at the instant of the impact), \dot{q}^- and \dot{q}^+ are, respectively, the velocity vectors just before and just after an inelastic impact. J_{f1} and J_{t2} characterize the contact of legs 1 and 2 with the ground during the impact, i_1 and i_2 are the wrenches corresponding to the impulsive forces and moments from the ground reaction acting on feet 1 and 2, respectively.

For the studied gaits, a finite-time double support phase is desired, thus for the first impact (Figs. 1(a) and (b)) one does not want the 1 foot to remain flat on the ground. Extensive simulations have shown that take-offs of the rear point foot can be avoided only if the landing velocity of the swing foot is zero [10] and therefore, there is no impact either. This solution has a high torque cost. Thus, in the following, it is assumed that only the toe of the rear foot remains on the ground after the impact. First, let us consider the walking motion 1. The swing foot hits the ground with a flat foot contact as shown in Fig. 1(a). In this case, the impact model is as follows:

$$D(q(T))(\dot{q}^+ - \dot{q}^-) = J_{f1}^T(q(T)) \begin{bmatrix} i_{1x} \\ i_{1y} \\ i_{\mathcal{M}1} \end{bmatrix} + J_{t2}^T(q(T)) \begin{bmatrix} i_{2x} \\ i_{2y} \end{bmatrix} \tag{4}$$

$$\begin{bmatrix} J_{f1}(q(T)) \\ J_{t2}(q(T)) \end{bmatrix} \dot{q}^+ = \mathbf{0}_{5 \times 1},$$

where the use of matrices J_{f1} and J_{t2} denotes that after impact the foot 1 has a foot flat contact with the ground and the foot 2 has a contact with the toe.

Let us consider now the walking motion 2. For one step, there are two impacts. The first impact occurs at the end of the single support phase when the swing foot heel impacts the ground, as shown in Fig. 2(a). This impact is described by the next equation:

$$\mathbf{D}(\mathbf{q}(T))(\dot{\mathbf{q}}^+ - \dot{\mathbf{q}}^-) = \mathbf{J}_{h1}^\top(\mathbf{q}(T)) \begin{bmatrix} i_{1x} \\ i_{1y} \end{bmatrix} + \mathbf{J}_{t2}^\top(\mathbf{q}(T)) \begin{bmatrix} i_{2x} \\ i_{2y} \end{bmatrix} \tag{5}$$

$$\begin{bmatrix} \mathbf{J}_{h1}(\mathbf{q}(T)) \\ \mathbf{J}_{t2}(\mathbf{q}(T)) \end{bmatrix} \dot{\mathbf{q}}^+ = \mathbf{0}_{4 \times 1},$$

where the use of matrices J_{h1} and J_{t2} denotes that after impact the foot 1 has a heel contact with the ground and the foot 2 has a toe contact with the ground. During the double support phase, the foot 2 rotates on its toe while the front foot rotates on its heel. The second impact occurs at the end of the double support phase, when the toe of the front foot reaches the ground and a flat-footed impact with the ground occurs while the rear foot takes off (see Fig. 2(c)). This second impact is described by the next equation:

$$\mathbf{D}(\mathbf{q}(T))(\dot{\mathbf{q}}^+ - \dot{\mathbf{q}}^-) = \mathbf{J}_{f1}^\top(\mathbf{q}(T)) \begin{bmatrix} i_{1x} \\ i_{1y} \\ i_{M1} \end{bmatrix} \tag{6}$$

$$\mathbf{J}_{f1}(\mathbf{q}(T))\dot{\mathbf{q}}^+ = \mathbf{0}_{3 \times 1}.$$

For each impact, when the velocity vector $\dot{\mathbf{q}}^-$ just before the impact is known, the resolution of the systems (4), (5), or (6) gives the velocity vector $\dot{\mathbf{q}}^+$ just after the impact and the impulsive reaction efforts \mathbf{i}_1 and \mathbf{i}_2 .

4. Gait optimization for the periodic walking

In this section, we present the algorithm for defining optimal walking trajectories. Each step of this algorithm has been carefully defined in order to minimize one sthenic criterion and to take into account all the physical and technological constraints that make walking possible. This is the core of our work.

To deal with a minimum energy walking, the Pontryagin’s principle can be used. This principle is used by Rostami and Besonnet [16] to design impactless walking motions for a seven-link planar biped robot with feet. However, the calculations are complex, the resulting equations are highly sensitive to the initial conditions, and this method generates bang–bang control laws [25]. Direct collocation method is an alternative to define walking motions. The principle of this method is to approach the solution of an ordinary differential equation or a partial differential equation for a finite set of points [13, 18, 26, 27, 28], and ref. [29]. The parametrization of the problem and the conversion of it into an algebraic optimization problem is another efficient alternative. Torques, Cartesian coordinates, or joint coordinates can be chosen to define the optimization parameters. Discrete values for the torques are used as optimization variables in ref. [30]. However, a numerical integration of the direct dynamic model is necessary to find the reference trajectory in velocity and position. To overcome this difficulty, the authors in refs. [31, 32], and [33] propose, respectively, polynomial functions and truncated Fourier series to approximate the temporal evolution of the joints, then torques are found through the algebraic solution of the inverse dynamic model. Cartesian coordinates are also convenient as optimization parameters [34], but this choice requires the use of inverse geometric model and for a given posture of the biped singularities can appear.

In this paper, a parametric optimization method is used and the evolution of a set of independent joint variables are expressed as polynomial functions of time. The coefficients of these polynomial functions define a set of desired initial, final, and intermediate positions and velocities. From the polynomial functions, we can calculate their first and second time derivatives. By using the inverse dynamic model, we can deduce the joint torques. A criterion based on the joint torques is minimized to define cyclic walking motions by considering optimization variables among the set coefficients of the polynomial functions.

4.1. Principle

The generalized coordinates of the biped are given by vector \mathbf{q} . However, these generalized coordinates are not independent due to the equation describing the contact with the ground. The locomotor system forms a geometrical closed loop with the ground. Thus, it is not possible to choose all these generalized coordinates arbitrarily. Among the set of generalized coordinates, several coordinates can be defined as function of time. The evolution of the other variables are then deduced based on geometrical relations that take into account the contact with the ground. The number of constraints varies with the phases of the motion (single support and finite-time double support).

Between two successive phases, the position and velocity of the biped must be continuous or the discontinuity must satisfy the impact Eqs. (4), (5), or (6). The set of parameters P specifying the cubic spline functions are determined by taking into account the transition conditions between the following phases.

The motion studied is assumed to be periodic and with the same behavior on support on legs 1 and 2. This periodic motion is designed with only one step. As consequence, the initial configuration at the beginning of the current step has to be deduced from the final configuration of the same step with a swapping role of the legs. Thus, assuming that the leg 1 is the stance leg in single support, an exchange of the number of the joints is carried out using a matrix \mathbf{A} as follows:

$$\mathbf{q}^+ = \mathbf{A}\mathbf{q}^-, \tag{7}$$

where

$$\mathbf{A} = \begin{bmatrix} 0 & 1 & 0 & 0 & 0 & 0 & 0 & 0 & 0 \\ 1 & 0 & 0 & 0 & 0 & 0 & 0 & 0 & 0 \\ 0 & 0 & 0 & 0 & 1 & 0 & 0 & 0 & 0 \\ 0 & 0 & 0 & 0 & 1 & 0 & 0 & 0 & 0 \\ 0 & 0 & 0 & 1 & 0 & 0 & 0 & 0 & 0 \\ 0 & 0 & 1 & 0 & 0 & 0 & 0 & 0 & 0 \\ 0 & 0 & 1 & 0 & 0 & 0 & 0 & 0 & 0 \\ 0 & 0 & 0 & 0 & 0 & 1 & 0 & 0 & 0 \\ 0 & 0 & 0 & 0 & 0 & 0 & 1 & 0 & 0 \\ 0 & 0 & 0 & 0 & 0 & 0 & 0 & 1 & 0 \\ 0 & 0 & 0 & 0 & 0 & 0 & 0 & 0 & 1 \end{bmatrix},$$

that is the initial configuration of the robot after the change of stance leg is the final configuration of the robot before the change of stance leg.

The set of optimization variables P minimizing a sthenic criterion are searched using a nonlinear optimization method. This algorithm is based on the calculation at each iteration of the gradient vector with respect to the optimization variables P , taking into account of nonlinear constraints. Physical conditions such as conditions of no slipping of the stance feet on the ground, of no unexpected contact with the ground of the transfer leg, and physical limits on the actuators define the nonlinear constraints in this optimization process.

4.1.1. The criterion

A lot of criteria can be used to produce an optimal trajectory. The cost transport (COT) to evaluate the biped gaits is a common and good option [35]. However, to deal with a smoother mathematical function, the sthenic criterion based on the squared torques is chosen to obtain optimal trajectories. As for a motor, its maximum delivered torque is strongly connected to its weight the physical meaning of this sthenic criterion is also interesting:

$$C_W = \frac{1}{d} \left(\int_0^T \mathbf{\Gamma}^\top \mathbf{\Gamma} dt \right) = \frac{1}{d} \left(\int_0^{T_{SS}} \mathbf{\Gamma}^\top \mathbf{\Gamma} dt + \int_{T_{SS}}^{T_{SS}+T_{DS}} \mathbf{\Gamma}^\top \mathbf{\Gamma} dt \right), \tag{8}$$

where T , T_{SS} , and T_{DS} are, respectively, the durations of the step, the single support phase, and the finite-time double support phase. Several motions with different velocities will be defined. When the walking

speed v is fixed, the step length d and T_{DS} are optimization variables. The step duration T is directly given through the relation $T = d/v$. Thus, we can deduce T_{SS} as follows:

$$T_{SS} = \frac{d}{v} - T_{DS}. \tag{9}$$

4.1.2. Parametric functions: Cubic spline

Cubic spline functions [36] are used to define the trajectories $\theta_i(t)$ of each independent angular variable during a phase of the walking motion,

$$\theta_i(t) = \begin{cases} \varphi_{i,1}(t) & \text{if } t_1 \leq t \leq t_2 \\ \varphi_{i,2}(t) & \text{if } t_2 \leq t \leq t_3 \\ \vdots & \\ \varphi_{i,n-1}(t) & \text{if } t_{n-1} \leq t \leq t_n. \end{cases} \quad i = 1, 2, \dots, n_j \tag{10}$$

Here, n is the number of selected knots and n_j is the number of angular variables. $\varphi_{i,1}(t), \dots, \varphi_{i,n-1}(t)$ are polynomials of third order such that:

$$\varphi_{i,k}(t) = \sum_{j=0}^3 a_{i,k}^j (t - t_k)^j, \text{ for } t \in [t_k, t_{k+1}], \quad k = 1, \dots, n - 1$$

where the coefficients $a_{i,k}^j$ are calculated such that the trajectory, velocity, and acceleration are continuous between t_1 and t_n . The cubic spline functions are uniquely defined by specifying an initial angular position $\theta_i(0)$, an initial angular velocity $\dot{\theta}_i(0)$ (both at $t = t_1 = 0$), a final angular position $\theta_i(T)$, and a final velocity $\dot{\theta}_i(T)$ (both at $t = t_n = T$), with T being the duration of the phase and $n - 2$ intermediate angular positions ($n - 2$ because let us recall that in finite-time double support and single support phases, the two Cartesian positions can be deduced from the knowledge of the angular positions). Consequently, the temporal joint evolution will be defined by a limited number of optimization parameters $((n + 2) \times n_j)$. When functions $\theta_i(t)$ are chosen, the joint velocities and accelerations can be deduced through time derivation of the polynomial function $\theta_i(t)$.

The number of parameters increases with the number of knots n but the order of the polynomial functions, the cubic spline functions does not increase. These cubic polynomials are sufficient to ensure the continuity of the second derivatives at nodes.

4.2. Description of the gait in the different phases

4.2.1. The single support phase

The biped has a foot contact flat on the ground, see Fig. 1(d) or Fig. 2(d). It means there are three unilateral constraints of contact in the stance foot with the ground. Thus, there are only $9 - 3 = 6$ independent generalized variables among the set of components of vector \mathbf{q} . Let us assume without loss of generality that the biped is in single support on foot 1. Then q_{f1}, \dot{q}_{f1} , and \ddot{q}_{f1} are null. We can choose as independent coordinates: $\Theta = [\theta_1, \theta_2, \theta_3, \theta_4, \theta_5, \theta_6]^T = [q_{f2}, q_1, q_2, q_3, q_4, q_5]^T$. The duration of the single support phase is $T_{SS} = T - T_{DS}$. The cubic spline functions $\theta_i(t)$, $i = 1, \dots, 6$ are defined with three selected knots, $n = 3$ for this phase. Thus, for each joint, we need to define five parameters of position and velocity to design the trajectories. If the single support phase is ended by a flat-footed impact of the swing leg, only four independent variables are necessary to define the final configuration of the robot. For the choice of these four independent variables we use the distance d between the front heel and the rear toe, see Fig. 6, the position coordinates of the hip x, y , and the inclination of the torso q_5 . If the single phase is ended by a heel impact of the swing leg, five independent generalized coordinates are

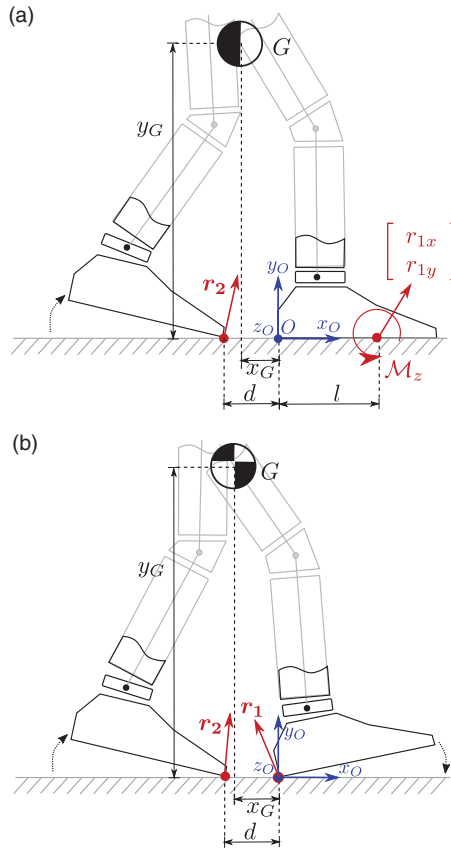


Figure 6. Ground reactions in double support phase and the center of mass of the biped. (a) DS of gait 1. (b) DS of gait 2.

necessary to define the final configuration of the robot. The angle of the front foot has to be added. The final velocity of the joints at the single support phase is described with six variables for both cases.

4.2.2. The finite-time double support phases

For gait 1, leg 1 has a flat foot contact and foot 2 rotates on its toe, as shown in Fig. 1(a). Then, there are five unilateral constraints of contact with the ground. There are nine generalized variables and five constraint equations. Thus, during the double support phase, the biped's configuration can be described with only four independent coordinates. Let us choose the orientation q_{f2} of foot 2, the orientation angles of leg 1 q_1, q_2 , and the inclination angle of the torso q_5 : $\Theta = [\theta_1, \theta_2, \theta_3, \theta_4]^T = [q_{f2}, q_1, q_2, q_5]^T$.

For gait 2, leg 1 rotates around its heel and foot 2 rotates on its toe, as shown in Fig. 2(a). Then there are four unilateral constraints of contact with the ground. There are nine generalized variables and four constraint equations. Thus, during the double support phase the biped's configuration can be described with only five independent coordinates. Let us choose: $\Theta = [\theta_1, \theta_2, \theta_3, \theta_4, \theta_5]^T = [q_{f1}, q_{f2}, q_1, q_2, q_5]^T$.

Let T_{DS} be the duration of the double support phase. Only limited evolution of the joints exists during the double support phase. Thus, the cubic spline functions $\theta_i(t)$, are defined with two selected knots for gait 1 and three for gait 2. We can remark that the distance between feet d is constant during this phase, thus the number of independent parameters to describe the robot configuration is reduced as it was shown.

Table II. Number of optimization variables for the walking gait 1.

Description	Optimization variables	Number of parameters
Final configuration of single support	$x_h(T_{SS}), y_h(T_{SS}), q_5(T_{SS})$	3
Final configuration of double support	$q_1(T_{DS}), q_2(T_{DS}), q_5(T_{DS}), q_{f2}(T_{DS})$	4
Intermediate configuration of single support	$q_{f2}(k \frac{T_{SS}}{n_{SS}-1}), q_1(k \frac{T_{SS}}{n_{SS}-1}), q_2(k \frac{T_{SS}}{n_{SS}-1}), q_3(k \frac{T_{SS}}{n_{SS}-1}), q_4(k \frac{T_{SS}}{n_{SS}-1}), q_5(k \frac{T_{SS}}{n_{SS}-1}), k = 1, \dots, n_{SS}-2$	$6(n_{SS}-2)$
Intermediate configuration of double support	$q_{f2}(k \frac{T_{DS}}{n_{DS}-1}), q_1(k \frac{T_{DS}}{n_{DS}-1}), q_2(k \frac{T_{DS}}{n_{DS}-1}), q_5(k \frac{T_{DS}}{n_{DS}-1})$ $k = 1, \dots, n_{DS} - 2$	$4(n_{DS}-2)$
Final velocities of single support	$\dot{q}_{f2}(T_{SS}), \dot{q}_1(T_{SS}), \dot{q}_2(T_{SS}), \dot{q}_3(T_{SS}), \dot{q}_4(T_{SS}), \dot{q}_5(T_{SS})$	6
Final velocities of double support	$\dot{q}_{f2}(T_{DS}), \dot{q}_1(T_{DS}), \dot{q}_2(T_{DS}), \dot{q}_5(T_{DS})$	4
Step length	d	1
Duration of double support	T_{DS}	1
Total		$4n_{DS} + 6n_{SS} - 1$

4.2.3. Continuity of the generalized coordinates between phases

The studied gaits are periodic, and the different phases are connected via impact model with a jump of velocities or continuity between the generalized coordinates, thus the initial configuration and velocity of each phase can be deduced based on the final configuration and velocity of the previous phase. The number of optimization variables can thus be reduced and are summarized in the Tables II and III. For the periodic walking motions 1 and 2, the number of knots for the single and double supports phases have been chosen in order to have similar number of optimization variables. For gait 1, we choose $n_{SS} = 4$ and $n_{DS} = 2$ that gives 31 optimization variables, and for gait 2, we choose $n_{SS} = 3$ and $n_{DS} = 3$ that gives 32 optimization variables. T_{DS} and d are also optimization variables. Taking into account Eq. (9), the duration of the single support phase T_{SS} can be deduced.

4.3. The optimal torque

When the motion of the biped is defined with the cubic functions as function of time (10), their first, and their second time derivatives can be calculated. The contact equation allows to define the vector \mathbf{q} of generalized coordinates and its derivatives $\dot{\mathbf{q}}$ and $\ddot{\mathbf{q}}$. Then the dynamic model (1) can be used to deduce the torque and the criterion can be evaluated. In the case of double support phase, due to actuation redundancy, many torques produce the same motion. A local optimal problem can be stated to choose the specific torques in double support as a function of the ground reaction. To define this calculation, we develop an explicit relation between the torque vector $\mathbf{\Gamma}$ and the wrench vector \mathbf{r}_2 . Then we detail both cases, double support phases and single support phases and show the associated constraints.

Table III. Number of optimization variables for the walking gait 2.

Description	Optimization variables	Number of parameters
Final configuration of single support	$x_h(T_{SS}), y_h(T_{SS}), q_5(T_{SS}), q_{f2}(T_{SS})$	4
Final configuration of double support	$q_1(T_{DS}), q_2(T_{DS}), q_5(T_{DS}), q_{f2}(T_{DS})$	4
Intermediate configuration of single support	$q_{f2}(k \frac{T_{SS}}{n_{SS}-1}), q_1(k \frac{T_{SS}}{n_{SS}-1}), q_2(k \frac{T_{SS}}{n_{SS}-1}), q_3(k \frac{T_{SS}}{n_{SS}-1}),$ $q_4(k \frac{T_{SS}}{n_{SS}-1}), q_5(k \frac{T_{SS}}{n_{SS}-1}), k = 1, \dots, n_{SS} - 2$	$6(n_{SS}-2)$
Intermediate configuration of double support	$q_{f1}(k \frac{T_{DS}}{n_{DS}-1}), q_{f2}(k \frac{T_{DS}}{n_{DS}-1}), q_1(k \frac{T_{DS}}{n_{DS}-1}), q_2(k \frac{T_{DS}}{n_{DS}-1}),$ $q_5(k \frac{T_{DS}}{n_{DS}-1}), k = 1, \dots, n_{DS} - 2$	$5(n_{DS}-2)$
Final velocities of single support	$\dot{q}_{f2}(T_{SS}), \dot{q}_1(T_{SS}), \dot{q}_2(T_{SS}), \dot{q}_3(T_{SS}), \dot{q}_4(T_{SS}), \dot{q}_5(T_{SS})$	6
Final velocities of double support	$\dot{q}_{f1}(T_{DS}), \dot{q}_{f2}(T_{DS}), \dot{q}_1(T_{DS}), \dot{q}_2(T_{DS}), \dot{q}_5(T_{DS})$	5
Step length	d	1
Duration of double support	T_{DS}	1
Total		$5n_{DS} + 6n_{SS} - 1$

4.3.1. Explicit relation between the torque vector Γ and the ground reaction in foot 2 \mathbf{r}_2

In finite-time double support phase, the locomotion system of the biped moves as a closed kinematic loop. This locomotion system is over-actuated. This situation requires an optimization process in order to manage the actuation redundancy and to find a solution that minimizes the criterion (8). This optimization process is based on an explicit relation between the torque vector Γ and the effort vector \mathbf{r}_2 . From the dynamic model (1), we can write both using the following equations:

$$\mathbf{B}^{\perp}(\mathbf{D}\ddot{\mathbf{q}} + \mathbf{N} + \mathbf{Q}) = \mathbf{B}^{\perp}(\mathbf{J}_1^{\top} \mathbf{r}_1 + \mathbf{J}_2^{\top} \mathbf{r}_2) \tag{11}$$

and

$$\mathbf{B}^+(\mathbf{D}\ddot{\mathbf{q}} + \mathbf{N} + \mathbf{Q}) = \Gamma + \mathbf{B}^+(\mathbf{J}_1^{\top} \mathbf{r}_1 + \mathbf{J}_2^{\top} \mathbf{r}_2). \tag{12}$$

Here, $\mathbf{B}^{\perp}(3 \times 9)$ and $\mathbf{B}^+(6 \times 9)$ are the orthogonal complement matrix and the pseudo-inverse matrix of \mathbf{B} , respectively, that is, $\mathbf{B}^{\perp}\mathbf{B} = \mathbf{0}_{3 \times 6}$, $\mathbf{B}^+\mathbf{B} = \mathbf{I}_{6 \times 6}$.

These Eqs. (11) and (12) will be used in the next subsection to manage the over actuation of the biped in finite-time double support and thus to manage an optimization of the torques in finite-time double support phase.

4.3.2. Optimal torques during the finite-time double support phase for gait 1

Let us first consider the gait 1, through the resultant wrench of the ground reaction, which is composed of two components for each force applied on both feet and one component for the moment vector on the

flat foot. The front leg has a flat foot contact (see Fig. 6(a)), thus the resultant wrench reaction of the ground acting in some point of this front foot is defined by $\mathbf{r}_1 = [r_{1x} \ r_{1y} \ \mathcal{M}_z]^\top$.

Let us consider the global equilibrium in translation and rotation of the biped, see Fig. 6(a). Let δ_g be the dynamic momentum of the biped with respect to its center of mass defined by the Cartesian coordinates (x_g, y_g) . We have five unknown variables, $\mathcal{M}_z, r_{1x}, r_{2x}, r_{1y}$, and r_{2y} for three equations only:

$$\begin{cases} y_g(r_{1x} + r_{2x}) + (x_g - d)r_{2y} + (x_g + l)r_{1y} + \mathcal{M}_z = \delta_g \\ r_{1x} + r_{2x} = m\ddot{x}_g \\ r_{1y} + r_{2y} - mg = m\ddot{y}_g. \end{cases} \tag{13}$$

Consequently, among $r_{1x}, r_{2x}, r_{1y}, r_{2y}$, and \mathcal{M}_z two variables can be chosen as optimization variables. For a given sum $r_{1x} + r_{2x}$, there are an infinity of solutions for r_{1y}, r_{2y} , and \mathcal{M}_z that satisfy the first and third equations of (13). Let r_{2x} and r_{2y} be the optimization variables. From (11) \mathbf{r}_1 is such as

$$\mathbf{r}_1 = (\mathbf{B}^\perp \mathbf{J}_1^\top)^{-1} \mathbf{B}^\perp (\mathbf{D}\ddot{\mathbf{q}} + \mathbf{N} + \mathbf{Q} - \mathbf{J}_2^\top \mathbf{r}_2), \tag{14}$$

assuming that $\mathbf{B}^\perp \mathbf{J}_1^\top$ is invertible as it has been tested in all our numerical tests.

Substituting \mathbf{r}_1 with its expression (14) in (12) the torque vector is such as

$$\begin{aligned} \boldsymbol{\Gamma} = & \mathbf{B}^+ (\mathbf{I}_{9 \times 9} - \mathbf{J}_1^\top (\mathbf{B}^\perp \mathbf{J}_1^\top)^{-1} \mathbf{B}^\perp) (\mathbf{D}\ddot{\mathbf{q}} + \mathbf{N} + \mathbf{Q}) - \\ & \mathbf{B}^+ (\mathbf{I}_{9 \times 9} - \mathbf{J}_1^\top (\mathbf{B}^\perp \mathbf{J}_1^\top)^{-1} \mathbf{B}^\perp) \mathbf{J}_2^\top \mathbf{r}_2. \end{aligned} \tag{15}$$

From Eq. (15), let us identify a linear relation, which emphasizes the effect of the optimization variable \mathbf{r}_2 on the actuated torque $\boldsymbol{\Gamma}$:

$$\boldsymbol{\Gamma} = \mathbf{M} - \mathbf{K} \mathbf{r}_2, \tag{16}$$

Here, the size of the matrices \mathbf{M}, \mathbf{K} is, respectively, (6×1) , and (6×2) and:

$$\begin{aligned} \mathbf{M} &= \mathbf{B}^+ (\mathbf{I}_{9 \times 9} - \mathbf{J}_1^\top (\mathbf{B}^\perp \mathbf{J}_1^\top)^{-1} \mathbf{B}^\perp) (\mathbf{D}\ddot{\mathbf{q}} + \mathbf{N} + \mathbf{Q}), \\ \mathbf{K} &= \mathbf{B}^+ (\mathbf{I}_{9 \times 9} - \mathbf{J}_1^\top (\mathbf{B}^\perp \mathbf{J}_1^\top)^{-1} \mathbf{B}^\perp) \mathbf{J}_2^\top. \end{aligned}$$

For a given motion we can locally choose the solution that minimizes the criterion (8),

$$\min_{r_{2x}, r_{2y}} \boldsymbol{\Gamma}^\top \boldsymbol{\Gamma}. \tag{17}$$

By using the relation (16) the expression of $\boldsymbol{\Gamma}^\top \boldsymbol{\Gamma}$ can be written as

$$\begin{aligned} \boldsymbol{\Gamma}^\top \boldsymbol{\Gamma} &= (\mathbf{M} - \mathbf{K} \mathbf{r}_2)^\top (\mathbf{M} - \mathbf{K} \mathbf{r}_2) \\ &= \mathbf{M}^\top \mathbf{M} - 2\mathbf{r}_2^\top \mathbf{K}^\top \mathbf{M} + \mathbf{r}_2^\top \mathbf{K}^\top \mathbf{K} \mathbf{r}_2. \end{aligned} \tag{18}$$

We have numerically checked that matrix $\mathbf{K}^\top \mathbf{K}$ is definite positive, thus the criterion $\boldsymbol{\Gamma}^\top \boldsymbol{\Gamma}$ as function of vector \mathbf{r}_2 is strictly convex and has a minimum. The solution $\mathbf{r}_{2\text{opt}}$ which minimizes $\boldsymbol{\Gamma}^\top \boldsymbol{\Gamma}$ can be calculated by writing that the derivative of $\boldsymbol{\Gamma}^\top \boldsymbol{\Gamma}$ with respect to \mathbf{r}_2 is equal to zero.

$$\begin{aligned} \frac{\partial}{\partial \mathbf{r}_2} (\boldsymbol{\Gamma}^\top \boldsymbol{\Gamma}) = 0 \Rightarrow \mathbf{r}_{2\text{opt}} &= (\mathbf{K}^\top \mathbf{K})^{-1} \mathbf{K}^\top \mathbf{M} \\ &= \mathbf{K}^+ \mathbf{M}. \end{aligned} \tag{19}$$

The solution $\mathbf{r}_{2\text{opt}} = [r_{2x\text{opt}} \ r_{2y\text{opt}}]^\top$ found with (19), minimizes $\boldsymbol{\Gamma}^\top \boldsymbol{\Gamma}$ without constraints.

Remark: For $\mathbf{r}_{2\text{opt}}$ the constraints of no take-off and no slipping in double support can be satisfied or not. At this stage of the optimization algorithm, we can search a solution \mathbf{r}_2 to satisfy the defined constraints. But another way, that we choose, is to reject the obtained global solution with the global optimization and the SQP optimization algorithm when a constraints is not satisfied.

4.3.3. Optimal torques during the double support phase for gait 2

For gait 2, the problem is similar but presents some differences. Let us consider the global equilibrium in translation and rotation of the biped (20), as shown in Fig. 6(b). The resultant reaction of the ground acting in the pivot point that represents the heel of the front foot 1 is defined by $\mathbf{r}_1 = [r_{1x} \ r_{1y}]^T$. Force $\mathbf{r}_2 = [r_{2x} \ r_{2y}]^T$ is the ground reaction acting in the toe of the rear foot 2, δ_g is the dynamic momentum of the biped with respect to its center of mass. We have four unknown variables, r_{1x} , r_{2x} , r_{1y} , and r_{2y} for three equations only.

$$\begin{cases} y_g(r_{1x} + r_{2x}) + (x_g - d)r_{2y} + x_g r_{1y} = \delta_g \\ r_{1x} + r_{2x} = m\ddot{x}_g \\ r_{1y} + r_{2y} - mg = m\ddot{y}_g. \end{cases} \tag{20}$$

For a given reference trajectory of the center of mass defined along with x_g , \dot{x}_g , and \ddot{x}_g , $m\ddot{x}_g$ is known, and then the sum $r_{1x} + r_{2x}$ through the second equation of (20). Consequently, r_{1y} and r_{2y} are the unique solution of the first and second equations of (20). But there are an infinity of solutions for r_{1x} or r_{2x} that satisfy the first and second equations of (20). Let r_{2x} be defined as an optimization variable to minimize locally the criterion (8). Using (11) we can write:

$$\begin{aligned} & \mathbf{B}^\perp(\mathbf{D}\ddot{\mathbf{q}} + \mathbf{N} + \mathbf{Q}) \\ &= \mathbf{B}^\perp \left(\mathbf{J}_1^T \begin{bmatrix} r_{1x} \\ r_{1y} \end{bmatrix} + \mathbf{J}_2^T \begin{bmatrix} r_{2x} \\ r_{2y} \end{bmatrix} \right), \\ &= \mathbf{B}^\perp \left(\mathbf{J}_1^T \begin{bmatrix} r_{1x} \\ r_{1y} \end{bmatrix} + \mathbf{J}_{21}^T r_{2x} + \mathbf{J}_{22}^T r_{2y} \right), \\ &= \mathbf{B}^\perp \left(\mathbf{J}_1^{\prime T} \begin{bmatrix} \mathbf{r}_1 \\ r_{2y} \end{bmatrix} + \mathbf{J}_{21} r_{2x} \right), \end{aligned} \tag{21}$$

with $\mathbf{J}_1^{\prime T} = [\mathbf{J}_1^T \ \mathbf{J}_{22}^T]$ and $\mathbf{r}_1 = [r_{1x} \ r_{2x}]^T$.

Assuming that $\mathbf{B}^\perp \mathbf{J}_1^{\prime T}$ is invertible (we observed that $\mathbf{B}^\perp \mathbf{J}_1^{\prime T}$ also is numerically invertible) we have:

$$\begin{bmatrix} \mathbf{r}_1 \\ r_{2y} \end{bmatrix} = (\mathbf{B}^\perp \mathbf{J}_1^{\prime T})^{-1} \mathbf{B}^\perp (\mathbf{D}\ddot{\mathbf{q}} + \mathbf{N} + \mathbf{Q} - \mathbf{J}_{21}^T r_{2x}). \tag{22}$$

From (12) we also can write:

$$\mathbf{B}^\perp(\mathbf{D}\ddot{\mathbf{q}} + \mathbf{N} + \mathbf{Q}) = \mathbf{\Gamma} + \mathbf{B}^+ \left(\mathbf{J}_1^{\prime T} \begin{bmatrix} \mathbf{r}_1 \\ r_{2y} \end{bmatrix} + \mathbf{J}_{21} r_{2x} \right). \tag{23}$$

Combining (22) with (23) we obtain:

$$\begin{aligned} \mathbf{\Gamma} &= \mathbf{B}^+(\mathbf{I}_{9 \times 9} - \mathbf{J}_1^{\prime T} (\mathbf{B}^\perp \mathbf{J}_1^{\prime T})^{-1} \mathbf{B}^\perp) (\mathbf{D}\ddot{\mathbf{q}} + \mathbf{N} + \mathbf{Q}) \\ &\quad - \mathbf{B}^+(\mathbf{I}_{9 \times 9} - \mathbf{J}_1^{\prime T} (\mathbf{B}^\perp \mathbf{J}_1^{\prime T})^{-1} \mathbf{B}^\perp) \mathbf{J}_{21}^T r_{2x}. \end{aligned} \tag{24}$$

From Eq. (24) let us identify the linear form in r_{2x} for $\mathbf{\Gamma}$:

$$\mathbf{\Gamma} = \mathbf{M}_1 - \mathbf{K}_1 r_{2x}. \tag{25}$$

Here, the size of the matrices \mathbf{M}_1 , \mathbf{K}_1 is (6×1) and:

$$\begin{aligned} \mathbf{M}_1 &= \mathbf{B}^+(\mathbf{I}_{9 \times 9} - \mathbf{J}_1^{\prime T} (\mathbf{B}^\perp \mathbf{J}_1^{\prime T})^{-1} \mathbf{B}^\perp) (\mathbf{D}\ddot{\mathbf{q}} + \mathbf{N} + \mathbf{Q}), \\ \mathbf{K}_1 &= \mathbf{B}^+(\mathbf{I}_{9 \times 9} - \mathbf{J}_1^{\prime T} (\mathbf{B}^\perp \mathbf{J}_1^{\prime T})^{-1} \mathbf{B}^\perp) \mathbf{J}_{21}^T. \end{aligned}$$

By using the same methodology that for the gait 1 with similar expressions to (18) and (19) the optimal solution is

$$\begin{aligned} \frac{\partial}{\partial r_{2x}}(\mathbf{\Gamma}^\top \mathbf{\Gamma}) &= 0 \\ \Rightarrow r_{2x \text{ opt}} &= \mathbf{K}_1^+ \mathbf{M}_1. \end{aligned} \tag{26}$$

Remarks:

- As the scalar term $\mathbf{K}_1^\top \mathbf{K}_1$ is strictly positive, $\mathbf{\Gamma}^\top \mathbf{\Gamma}$ as function of r_{2x} has a minimum.
- Similarly to gait 1 if $r_{2x \text{ opt}}$ does not satisfy the constraints of no take-off and no slipping, the SQP optimization algorithm will reject the obtained solution in the global optimization.

4.4. Parametric optimization problem

By parameterizing the joint motion in terms of cubic spline functions, the optimization problem is reduced to a constrained parametric optimization problem of the form:

$$\begin{aligned} \text{Minimize } C_W(\mathbf{P}) \\ \text{subject to } \mathbf{g}_j(\mathbf{P}) \leq 0 \text{ for } j = 1, 2, \dots, l \end{aligned} \tag{27}$$

where \mathbf{P} is the set of optimization variables. $C_W(\mathbf{P})$, which is the sthenic criterion (8), is minimized with l inequality constraints $\mathbf{g}_j(\mathbf{P}) \leq 0$ to satisfy. The vector $\mathbf{g}_j(\mathbf{P}) \leq 0$ regroups the unilateral constraints of contact with ground reactions, the geometrical constraints and motor limits. The criterion and these constraints are given in the following sections.

4.4.1. The single support phase

The biped has a flat foot contact on the ground, as shown in Fig. 1(c). The resultant wrench of the ground reaction is composed of two components for the force and one component for the moment. In the second foot the resultant wrench of the ground reaction is null (assuming that the stance foot is foot 1, $r_2 = 0$).

The dynamic model (1) becomes:

$$\mathbf{D}\ddot{\mathbf{q}} + \mathbf{N} + \mathbf{Q} = \mathbf{B}\mathbf{\Gamma} + \mathbf{J}_1^\top \mathbf{r}_1. \tag{28}$$

By knowing $\mathbf{q}, \dot{\mathbf{q}}, \ddot{\mathbf{q}}$, which satisfy (2), this matrix equation has a unique solution for the torque vector $\mathbf{\Gamma}$ and the ground reaction effort \mathbf{r}_1 .

4.4.2. The constraints

Two types of constraints are used to obtain a realistic gait.

- The contact constraints, which ensure a valid walking. The first constraint ensures the stance leg does not take off or slide on the ground. The vertical component of the ground reaction of the foot must be positive. Furthermore, the ground reaction force is inside a friction cone, defined with the coefficient of friction μ_f :

$$\begin{cases} -r_{jy} < 0 \\ (-\mu_f r_{jy} - r_{jx}) \leq 0 \\ (-\mu_f r_{jy} + r_{jx}) \leq 0, \end{cases} \tag{29}$$

$j = 1$ and/or 2 . r_{jx} and r_{jy} are the normal and tangential components of the reaction force. Moreover, we can introduce a constraint on the ground reaction at the impact:

$$\begin{cases} -i_{jy} < 0 \\ (-\mu_f i_{jy} - i_{jx}) \leq 0 \\ (-\mu_f i_{jy} + i_{jx}) \leq 0, \end{cases} \tag{30}$$

Table IV. Actuator limits in torques and velocities.

	Hip joint	Knee joint	Ankle joint
Maximum torque (N.m)	30	10	20
Maximum velocity (rad/s)	6	10	20
Maximum power (W)	180	100	300

$j = 1$ and/or 2 . We choose an arbitrary numerical value for the friction coefficient μ_f equals to 0.7 . To ensure the non-rotation of the stance flat foot we introduce a constraint on the *ZMP* during contact phase and at the instant of the impact:

$$-l_f \leq l_{ZMP} \leq L_f - l_f. \tag{31}$$

l_{ZMP} represents the distance between the *ZMP* and the projection of the ankle joint on the ground, see Fig. 5.

Just after the impact, the velocity of the taking-off foot should be directed upward. As a consequence, the positivity of the vertical component of the velocities for the heel and the toes is added to the set of constraints.

The next constraint allows to ensure the nonpenetration of the swinging foot in the ground. Defining the altitude of the toe and the heel of the foot 2 from expressions in Appendix we obtain inequality constraints as follows:

$$\begin{aligned}
 y - l_2 \cos q_3 - l_1 \cos q_4 + (L_f - l_f) \sin q_{f2} - H_f \cos q_{f2} &\geq 0, \\
 \text{and} \\
 y - l_2 \cos q_3 - l_1 \cos q_4 - l_f \sin q_{f2} - H_f \cos q_{f2} &\geq 0.
 \end{aligned}
 \tag{32}$$

- The geometrical constraints and actuator limits to ensure a technological realistic gait: For the joint variables of the knee, we limit the domain of desired solutions such as the knee counterflexion is avoided. Moreover, Table IV gathers the motor limits in torque, velocity, and power for the joints of the hips, knees, and the ankles. These maximum values, are those of the locomotor system of the hydroid robot, which the power supply fluid is hydraulic. They are used for the two gaits and for each velocity of the optimal walking.

A block diagram that summarize the parametric optimization algorithm proposed in this paper to define the two gaits is described in Fig 7.

5. Optimal walking: simulation results

The problem of parametric minimization with constraints to obtain the optimal walking is numerically solved, using the *SQP* method see refs. [37] and [38] with the *fmincon* function of Matlab ®. Figure 8 shows the cost criterion as function of the walking velocity of the biped for both gaits. The choice of the initial conditions for the optimization process is very important. The described curves are the results of several iterative optimization tests, by adapting the initial conditions for the current velocity from the previous velocity, starting from the lower or the higher allowable speed. For the gait 1, a cyclic motion has been found for walking velocity between 0.22 m/s and 1 m/s. The criterion has a minimum around 0.36 m/s. The energy increases quasi linearly for higher walking velocities. For gait 2, the optimization algorithm does not converge outside the velocity interval [0.5 m/s, 0.94 m/s]. However, walking velocities faster than 0.55 m/s have values of the cost criterion lower than those obtained with the gait 1. In the sense of speed walking, a synchronized rotation of both feet during the double support phase is more efficient than a flat foot contact on ground and a rotation around the toe of the other foot. We observed with numerical results that for both gaits with the impact model (3) at the end of the single support the velocity of the landing foot is small. This is in agreement with the numerical analyze made by Miossec

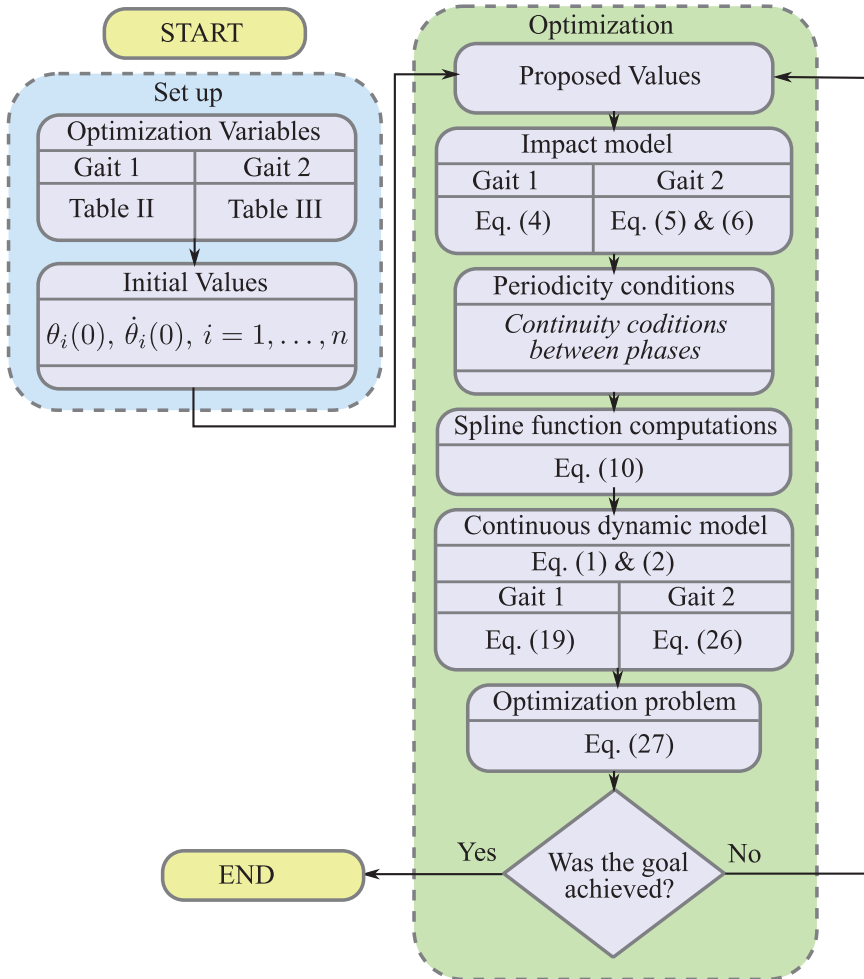


Figure 7. Block diagram of the parametric optimization for defining the two gaits.

and Aoustin [39]. The reason is that, it is very difficult to include a finite-time double support after a discontinuity of the velocity of the landing foot and simultaneously to satisfy the unilateral constraints of friction and no take-off with an absolutely inelastic impact model.

Figure 8 shows the ranges of feasible speeds for both gaits 1 and 2. Outside the speed ranges, the actuators can no longer provide enough power to perform the operation or the optimization algorithm cannot find a solution, which satisfies the unilateral constraints of the biped robot with the ground. The speed range is larger for the gait 1 than for the gait 2. However, for the common domain of both gaits, the sthenic criterion is weaker for the 2 gait, especially around the comfort speed of a healthy adult human, that is almost equal to 4.4 km/h ± 0.8, [40]. This fact leads us to believe that gait 2 is more anthropomorphic than gait 1. Parametric optimization by definition provides a minimal solution of a criterion that is not an optimal solution in the Pontryagin sense. In reality for each speed, with another criterion, another strategy for choosing the initial value of the optimized variables, different written of the constraints, it may be possible to find a different robot motion. However, the multiple numerical tests that led us to these results, proved that the following general trend is true regardless of the trajectory calculation method: Gait 1 is better at low speed and worse at high speed than gait 2. From Fig. 8, we choose the velocity 0.9 m/s (3.24 km/h) to detail the walking for both gaits. This is not far from the

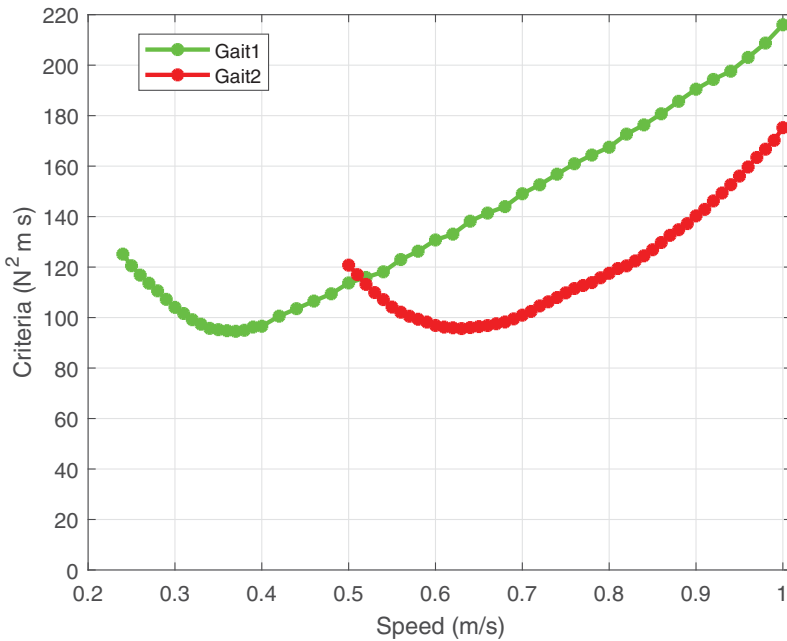


Figure 8. Cost criterion as function of the walking velocity for gait 1 (green) and gait 2 (red).

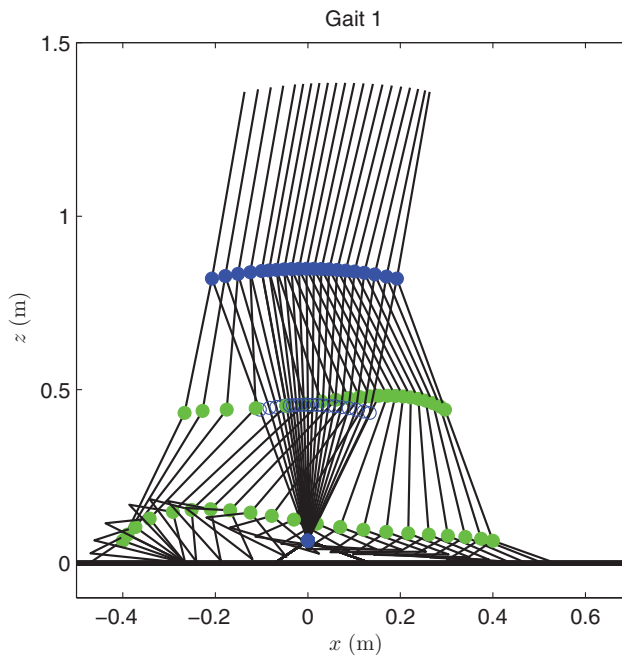


Figure 9. Stick diagram of the gait 1.

comfort velocity. Figures 9 and 10 describe a stick diagram for one step of the walking motion with gaits 1 and 2, respectively.

Figure 11 presents the orientation variables of the feet for gait 1. We can observe the flat foot contact of the stance foot on the ground. The value of the orientation of its sole is null with respect to the ground.

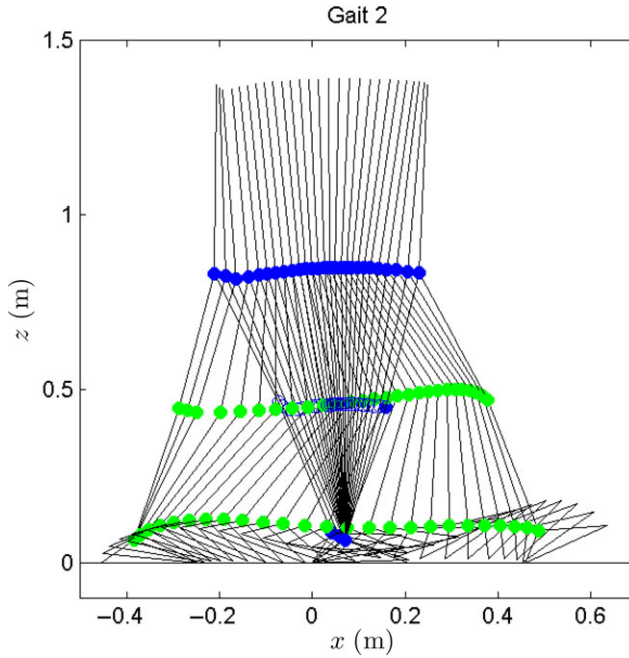


Figure 10. Stick diagram of the gait 2.

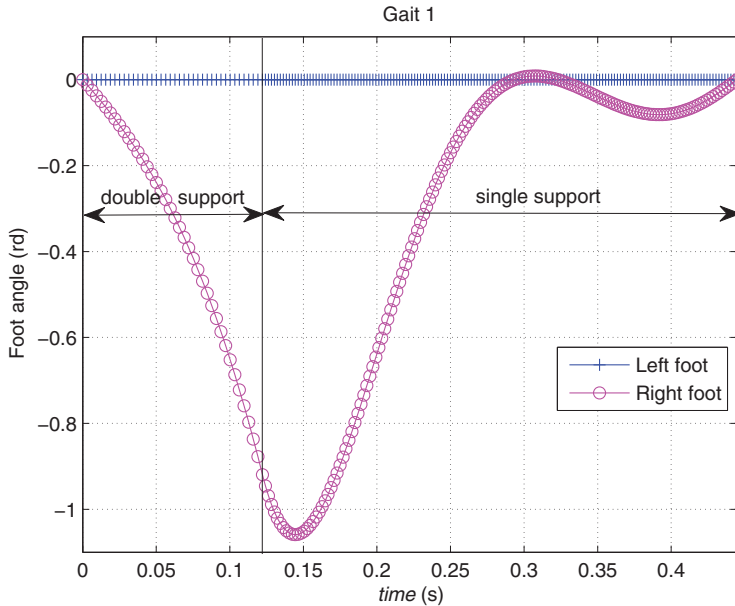


Figure 11. Profile of the foot orientations with respect to the ground for the gait 1.

Figure 12 shows the profile of the torques and, the discontinuities of the torques, allows us to discern the impact at $t = 0$, and the transition between the double support phase and the single support phase, which occurs at 0.12 s. The profile of the torques show a discontinuity at the impact ($t = 0$) because there is a jump of velocities, which is coherent with the definition of the gait 1. During the double support phase, the rear foot rotates around its toe until 0.12 s and after it becomes the swing foot.

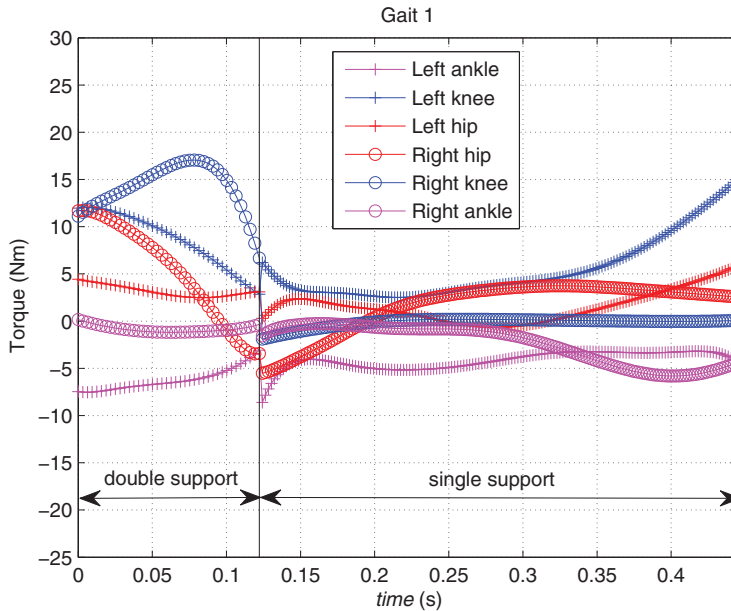


Figure 12. Profile of the torques for the gait 1.

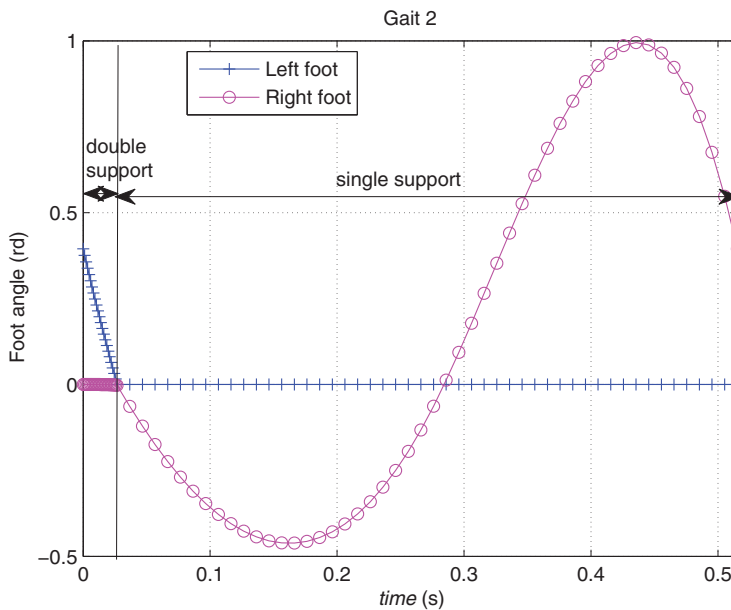


Figure 13. Profile of the foot orientations with respect to the ground for the gait 2.

Figure 13 presents the orientation variables of the feet for gait 2. We can explicitly see the end of the finite-time double support phase. The front foot rotates around its heel until 0.04 s when the orientation of its sole is null. The orientation value of the rear foot is almost zero during the double support phase; however, the numerical results prove that there is a small rotation of this foot around its toe. After the impact of the front feet, the rear foot becomes the swing foot and its rotation increases. Figure 14 shows the profile of the torques and, at the discontinuities of the torques, the transition between phases. Similarly to gait 1, the profile of the torques show a discontinuity at the impacts because there is a jump

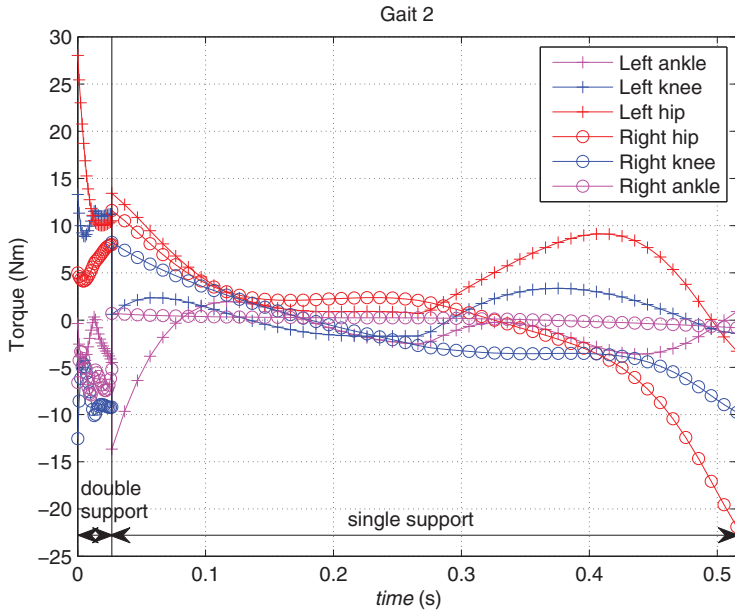


Figure 14. Profile of the torques for the gait 2.

of velocities, that is also coherent with the definition of this gait 2. The time duration of the double support phase, which is an optimization variable, for the gait 2 is smaller than for the gait 1. It could be a reason why the consumption of energy is less for the gait 2 than for the gait 1 because the motion of the swing leg is quasi ballistic [41].

6. Conclusion

This paper deals with the design of optimal periodic walking motions with finite-time double support phases and single support phases for a planar biped through a parametric optimization. The three original main results of this numerical study are the following. First, with the algebraic model of impact, the fact to accept a rotation of the rear foot on its toe, which was the previous stance foot in single support, allows to get a valid noninstantaneous double support phase. That means this model satisfies the unilateral constraints that is the vertical component of the impulsive ground reaction is positive for the two feet and the tangential force is in the friction cone. It is true for all the calculated walking motions for a landing of the swing foot on its heel or with flat foot contact. Second, the range of allowable speeds is greater for the finite-time double support phase where the swing foot is landing with a flat foot contact on the ground than for the finite double support phase that allows a synchronized rotation of both feet. For both kinds of finite-time double support phases, beyond the upper and lower limits in speeds, the optimization algorithm cannot find any optimal solution, which satisfies the unilateral constraints. Third, the gait 1, which has a flat foot contact in finite-time double support phase, is optimal for the low velocities. The gait 2, which allows a rotation of both feet, is optimal for high biped speeds. This last result is coherent with the observations of the biomechanical data from several researchers in biomechanics [42].

The developed tools here could be useful in the design of a prosthesis or an exoskeleton for rehabilitation, specially to tune the assistance for the locomotor system. Walking motion designed for healthy people can be defined as a reference motion to track for handicapped people by tuning the assistance of the prosthesis or the exoskeleton during the gait. Preliminary results can be found in ref. [43].

Note

1 Sign \top means transposed vector or transposed matrix in this paper.

References

- [1] R. Alexander, "The gaits of bipedal and quadrupedal animals," *Int. J. Rob. Res.* **3**(4), 49–59 (1984).
- [2] R. Singh, H. Chaudhary and A. K. Singh, *Sagittal Position Analysis of Gait Cycle for a Five Link Biped Robot* (Springer, 2016) pp. 387–396.
- [3] J. Saunders, T. I. Verne and D. E. Howard, "The major determinants in normal and pathological gait," *J. Bone Joint Surg.* **35**(3), 543–558 (1953).
- [4] D. Winter, *Biomechanics and Motor Control of Human Movement* (John Wiley & Sons, Inc., Hoboken, NJ, 2005).
- [5] C. Chevallereau, G. Bessonnet, G. Abba and Y. Aoustin, *Bipedal Robots* (ISTE Wiley, London, 2009).
- [6] S. Nadubettu Yadukumar, M. Pasupuleti and A. Ames, "Human-Inspired Underactuated Bipedal Robotic Walking with Amber on Flat-Ground, Up-Slope and Uneven Terrain," *IEEE/RSJ International Conference on Intelligent Robots and Systems*, Vilamoura, Algarve, Portugal (2012).
- [7] C. Chevallereau, G. Abba, Y. Aoustin, F. Plestan, E. Westervelt, C. Canuddas-de Wit and J. Grizzle, "Rabbit: A testbed for advanced control theory," *IEEE Control Syst. Mag.* **23**(5), 57–79 (2003).
- [8] S. Kajita, F. Kanehiro, M. Morisawa, S. Nakaoka and H. Hirukawa, "Biped Walking Pattern Generator Allowing Auxiliary ZMP Control," *2006 IEEE/RSJ International Conference on Intelligent Robots and Systems*, Beijing, P.R. China (2006) pp. 2993–2999.
- [9] S. Omran, S. Sakka and Y. Aoustin, "Effects of com vertical oscillation on joint torques during 3D walking of humanoid robots," *Int. J. Hum. Rob.* **13**(4), 1650019 (2016). <https://doi.org/10.1142/S02198436165001951650019>.
- [10] S. Miossec and Y. Aoustin, "A simplified stability for a biped walk with under and over actuated phase," *Int. J. Rob. Res.* **24**(7), 537–551 (2005).
- [11] K. K. Hamed, N. Sadati, W. A. Gruver and G. A. Dumont, "Stabilization of periodic orbits for planar walking with noninstantaneous double-support phase," *IEEE Trans. Syst. Man Cybern. Part A Syst. Hum.* **42**(3), 685–706 (2012).
- [12] M. S. Ju and J. M. Mansour, "Simulation of the double limb support phase of human gait," *J. Biomech. Eng.* **110**(3), 223–229 (1988).
- [13] N. Sharma and R. Stein, "Gait Planning and Double Support Phase Model for Functional Electrical Stimulation-based Walking," *33th Annual International Conference of the IEEE EMBS*, San Diego, California USA (2012).
- [14] G. Bessonnet, S. Chesse and P. Sardain, "Optimal gait synthesis of a seven-link planar biped," *Int. J. Rob. Res.* **23**(10–11), 1059–1073 (2004).
- [15] D. Tlalolini Romero, C. Chevallereau and Y. Aoustin, "Comparison of different gaits with rotation of the feet for a planar biped," *Rob. Auto. Syst.* **57**(4), 371–383 (2009).
- [16] M. Rostami and G. Bessonnet, "Impactless Sagittal Gait of a Biped Robot During the Single Support Phase," *IEEE International Conference on Robotics and Automation ICRA'98*, Leuven, Belgium (1998).
- [17] Y. Aoustin and A. Hamon, "Human like trajectory generation for a biped robot with a four-bar linkage for the knees," *Rob. Auto. Syst.* **61**(12), 1717–1725 (2013).
- [18] M. Tan, L. Jennings and S. Wang, *Analysing Human Walking Using Dynamic Optimisation* (Springer, Berlin, Heidelberg, 2015) pp. 1–34.
- [19] D. Dadashzadeh and C. J. B. Macnab, "Slip-based control of bipedal walking based on two-level control strategy," *Robotica* **38**(8), 1434–1449 (2020).
- [20] T. Kinugasa, C. Chevallereau and Y. Aoustin, "Effect of circular arc feet on a control law for a biped," *Robotica* **27**(4), 621–632 (2009).
- [21] S. Bertrand, O. Bruneau, F. B. Ouedzou and S. Alfayad, "Closed-form solutions of inverse kinematic models for the control of a biped robot with 8 active degrees of freedom per leg," *Mech. Mach. Theory*, Elsevier **49** 117–140 (2012).
- [22] C. Chevallereau and Y. Aoustin, "Optimal reference trajectories for walking and running of a biped robot," *Robotica* **19**(5), 557–569 (2001).
- [23] S. Alfayad, Robot humanoïde hydroïd: Actionnement structure cinématique et stratégie de contrôle *Ph.D. Thesis* (Université de Versailles Saint-Quentin, 2009).
- [24] E. P. Hanavan, "A personalized mathematical model of the human body," *J. Spacecraft Rockets* **3**(3), 446–448 (1966).
- [25] A. E. Bryson and Y. C. Ho, *Applied Optimal Control* (Wiley, New-York, 1995).
- [26] G. Vainikko, "On the stability and convergence of the collocation method," *Differ. Uravnen.* **1**(2), 244–254 (1965).
- [27] M. K. El Daou and E. L. Ortiz, "A recursive formulation of collocation in terms of caical polynomials," *Comput.* **52**(2), 177–202 (1994).
- [28] K. Mombaur, H. G. Bock, J. P. Schlöder and R. W. Longman, "Open-loop stable solutions of periodic optimal control problems in robotics," *ZAMM* **85**(7), 499–515 (2005).
- [29] F. D. Groote, A. L. Kinney, A. V. Rao and B. J. Fregly, "Evaluation of direct collocation optimal control problem formulations for solving the muscle redundancy problem," *Ann. Biomed. Eng.* **44**(10), 2922–2936 (2016).

[30] L. Roussel, C. C. de Wit and A. Goswami, "Generation of Energy Optimal Complete Gait Cycles for Biped," *Proceedings of the IEEE Conference on Robotics and Automation* (1998) pp. 2036–2041.

[31] V. V. Beletskii and P. S. Chudinov, "Parametric optimization in the problem of bipedal locomotion," *Izv. An SSSR. Mekhanika Tverdogo Tela [Mech. Solids]* **12**(1), 25–35 (1977).

[32] P. H. Channon, S. H. Hopkins and D. T. Pham, "Derivation of optimal walking motions for a bipedal walking robot," *Robotica* **10**(3), 165–172 (1992).

[33] G. Cabodevilla, N. Chaillet and G. Abba, "Energy-Minimized Gait for a Biped Robot," *Proceedings of the AMS'95*, Tampa, Florida, USA (2002) pp. 90–99.

[34] Q. Huang, K. Yokoi, S. Kajita, K. Kaneko, H. Arai, N. Koyachi and K. Tanie, "Planning walking patterns for a biped robot," *IEEE Trans. Rob. Autom.* **17**(3), 280–289 (2001).

[35] D. Roberts, J. Quacinella and J. H. Kim, "Energy expenditure of a biped walking robot: Instantaneous and degree-of-freedom-based instrumentation with human gait implications," *Robotica* **35**(5), 1054–1071 (2017).

[36] C. D. Boor, *A Practical Guide to Splines. Applied Mathematical Sciences* (Springer-Verlag, New York, 1978).

[37] P. Gill, W. Murray and M. Wright, *Practical Optimization* (Academic Press, London, 1981).

[38] M. Powell, *Variable Metric Methods for Constrained Optimization, Lecture Notes in Mathematics* (Springer, Berlin, Heidelberg, 1977) pp. 62–72.

[39] S. Miossec and Y. Aoustin, *Dynamical Synthesis of a Walking Cyclic Gait for a Biped with Point Feet, Lecture Notes in Control and Information Sciences*, vol. 340 (Springer, Berlin, Heidelberg, 2006) pp. 233–252.

[40] J. Cottalorda, C. Durst, R. Aubail, A. Belli and V. Gautheron, Geysant, "Consommation énergétique à la vitesse de confort au sol et sur tapis roulant," *Annales de Réadaptation et de Médecine Physique, Editions scientifiques et médicales*, Elsevier **43**(1), 30–35 (2000).

[41] S. Mochon and T. McMahon, Ballistic walking: An improved model," *Math. Bio-Sci.* **52**(3–4), 241–260 (1980).

[42] J. Rose and G. Gamble, *Human Walking*, 3rd edn. (Lippincott Williams & Wilkins, Philadelphia, PA, 2006). p. 273.

[43] Y. Aoustin, C. Chevallereau and V. Arakelian, "Study and Choice of Actuation for a Walking Assist Device," *In: New Trends in Medical and Service Robots. Mechanisms and Machine Science, Vol. 38* (H. Bleuler, M. Bouri, F. Mondada, D. Pisla, A. Rodic and P. Helmer, eds.) (Springer, Cham, 2016). https://doi.org/10.1007/978-3-319-23832-6_1.

Appendix

A.1. The Equations of Contact with the Ground for the Biped in Position, Velocity, and Acceleration

Equations for legs 1 and 2 are similar with different joint variables. For a sake of clarity we consider leg 1 only.

- Contact with the heel

$$\begin{aligned} x + l_2 \sin q_2 + l_1 \sin q_1 - l_f \cos q_{f1} + H_f \sin q_{f1} &= \text{const}, \\ y - l_2 \cos q_2 - l_1 \cos q_1 - l_f \sin q_{f1} - H_f \cos q_{f1} &= 0. \end{aligned} \tag{A1}$$

The first time derivative of (A1) is

$$\begin{aligned} \dot{x} + l_2 \dot{q}_2 \cos q_2 + l_1 \dot{q}_1 \cos q_1 + l_f \dot{q}_{f1} \sin q_{f1} + \\ H_f \dot{q}_{f1} \cos q_{f1} &= 0, \\ \dot{y} + l_2 \dot{q}_2 \sin q_2 + l_1 \dot{q}_1 \sin q_1 - l_f \dot{q}_{f1} \cos q_{f1} + \\ H_f \dot{q}_{f1} \sin q_{f1} &= 0. \end{aligned} \tag{A2}$$

In compact form (A2) becomes: $\mathbf{J}_{h1} \dot{\mathbf{q}} = \mathbf{0}$ with

$$\mathbf{J}_{h1} = \begin{bmatrix} l_f \sin q_{f1} + H_f \cos q_{f1} & 0 & l_1 \cos q_1 & l_2 \cos q_2 & 0 & 0 & 0 & 1 & 0 \\ -l_f \cos q_{f1} + H_f \sin q_{f1} & 0 & l_1 \sin q_1 & l_2 \sin q_2 & 0 & 0 & 0 & 0 & 1 \end{bmatrix}. \tag{A3}$$

The second time derivative of (A1) is

$$\begin{aligned} \ddot{x} + l_2\ddot{q}_2 \cos q_2 + l_1\ddot{q}_1 \cos q_1 + l_f\ddot{q}_{f1} \sin q_{f1} + \\ H_f\ddot{q}_{f1} \cos q_{f1} - l_2\dot{q}_2^2 \sin q_2 - l_1\dot{q}_1^2 \sin q_1 + \\ l_f\dot{q}_{f1}^2 \cos q_{f1} - H_f\dot{q}_{f1}^2 \sin q_{f1} = 0, \\ \ddot{y} + l_2\ddot{q}_2 \sin q_2 + l_1\ddot{q}_1 \sin q_1 - l_f\ddot{q}_{f1} \cos q_{f1} + \\ H_f\ddot{q}_{f1} \sin q_{f1} + l_2\dot{q}_2^2 \cos q_2 + l_1\dot{q}_1^2 \cos q_1 + \\ l_f\dot{q}_{f1}^2 \sin q_{f1} + H_f\dot{q}_{f1}^2 \cos q_{f1} = 0. \end{aligned} \tag{A4}$$

In compact form (A4) becomes: $\mathbf{J}_{h1}\ddot{\mathbf{q}} + \dot{\mathbf{J}}_{h1}\dot{\mathbf{q}} = \mathbf{0}$.

- Contact with the toe

$$\begin{aligned} x + l_2 \sin q_2 + l_1 \sin q_1 + (L_f - l_f) \cos q_{f1} + H_f \sin q_{f1} = const, \\ y - l_2 \cos q_2 - l_1 \cos q_1 + (L_f - l_f) \sin q_{f1} - H_f \cos q_{f1} = 0. \end{aligned} \tag{A5}$$

The first time derivative of (A5) is

$$\begin{aligned} \dot{x} + l_2\dot{q}_2 \cos q_2 + l_1\dot{q}_1 \cos q_1 - (L_f - l_f)\dot{q}_{f1} \sin q_{f1} + \\ H_f\dot{q}_{f1} \cos q_{f1} = 0, \\ \dot{y} + l_2\dot{q}_2 \sin q_2 + l_1\dot{q}_1 \sin q_1 + (L_f - l_f)\dot{q}_{f1} \cos q_{f1} + \\ H_f\dot{q}_{f1} \sin q_{f1} = 0. \end{aligned} \tag{A6}$$

In compact form (A6) becomes: $\mathbf{J}_{t1}\dot{\mathbf{q}} = \mathbf{0}$ with

$$\mathbf{J}_{t1} = \begin{bmatrix} -(L_f - l_f) \sin q_{f1} + \\ H_f \cos q_{f1} & 0 & l_1 \cos q_1 & l_2 \cos q_2 & 0 & 0 & 0 & 1 & 0 \\ (L_f - l_f) \cos q_{f1} + \\ H_f \sin q_{f1} & 0 & l_1 \sin q_1 & l_2 \sin q_2 & 0 & 0 & 0 & 0 & 1 \end{bmatrix}. \tag{A7}$$

The second time derivative of (A5) is

$$\begin{aligned} \ddot{x} + l_2\ddot{q}_2 \cos q_2 + l_1\ddot{q}_1 \cos q_1 - (L_f - l_f)\ddot{q}_{f1} \sin q_{f1} + \\ H_f\ddot{q}_{f1} \cos q_{f1} - l_2\dot{q}_2^2 \sin q_2 - l_1\dot{q}_1^2 \sin q_1 - \\ (L_f - l_f)\dot{q}_{f1}^2 \cos q_{f1} - H_f\dot{q}_{f1}^2 \sin q_{f1} = 0, \\ \ddot{y} + l_2\ddot{q}_2 \sin q_2 + l_1\ddot{q}_1 \sin q_1 + (L_f - l_f)\ddot{q}_{f1} \cos q_{f1} + \\ H_f\ddot{q}_{f1} \sin q_{f1} + l_2\dot{q}_2^2 \cos q_2 + l_1\dot{q}_1^2 \cos q_1 - \\ (L_f - l_f)\dot{q}_{f1}^2 \sin q_{f1} + H_f\dot{q}_{f1}^2 \cos q_{f1} = 0. \end{aligned} \tag{A8}$$

In compact form (A8) becomes: $\mathbf{J}_{t1}\ddot{\mathbf{q}} + \dot{\mathbf{J}}_{t1}\dot{\mathbf{q}} = \mathbf{0}$.

- Flat foot contact

$$\begin{aligned} x + l_2 \sin q_2 + l_1 \sin q_1 + H_f \sin q_{f1} &= \text{const}, \\ y - l_2 \cos q_2 - l_1 \cos q_1 - H_f \cos q_{f1} &= 0. \end{aligned} \tag{A9}$$

$$q_{f1} = 0$$

The first time derivative of (A9) is

$$\begin{aligned} \dot{x} + l_2 \dot{q}_2 \cos q_2 + l_1 \dot{q}_1 \cos q_1 + H_f \dot{q}_{f1} \cos q_{f1} &= 0 \\ \dot{y} + l_2 \dot{q}_2 \sin q_2 + l_1 \dot{q}_1 \sin q_1 + H_f \dot{q}_{f1} \sin q_{f1} &= 0. \end{aligned} \tag{A10}$$

$$\dot{q}_{f1} = 0$$

In compact form (A10) becomes: $\mathbf{J}_{f1} \dot{\mathbf{q}} = \mathbf{0}$

$$\mathbf{J}_{f1} = \begin{bmatrix} H_f \cos q_{f1} & 0 & l_1 \cos q_1 & l_2 \cos q_2 & 0 & 0 & 0 & 1 & 0 \\ H_f \sin q_{f1} & 0 & l_1 \sin q_1 & l_2 \sin q_2 & 0 & 0 & 0 & 0 & 1 \\ 1 & 0 & 0 & 0 & 0 & 0 & 0 & 0 & 0 \end{bmatrix}. \tag{A11}$$

The second time derivative of (A9) is

$$\begin{aligned} \ddot{x} + l_2 \ddot{q}_2 \cos q_2 + l_1 \ddot{q}_1 \cos q_1 + H_f \ddot{q}_{f1} \cos q_{f1} - \\ l_2 \dot{q}_2^2 \sin q_2 - l_1 \dot{q}_1^2 \sin q_1 - H_f \dot{q}_{f1}^2 \sin q_{f1} &= 0, \\ \ddot{y} + l_2 \ddot{q}_2 \sin q_2 + l_1 \ddot{q}_1 \sin q_1 + H_f \ddot{q}_{f1} \sin q_{f1} + \\ l_2 \dot{q}_2^2 \cos q_2 + l_1 \dot{q}_1^2 \cos q_1 + H_f \dot{q}_{f1}^2 \cos q_{f1} &= 0. \end{aligned} \tag{A12}$$

$$\ddot{q}_{f1} = 0$$

In compact form (A12) becomes: $\mathbf{J}_{f1} \ddot{\mathbf{q}} + \dot{\mathbf{J}}_{f1} \dot{\mathbf{q}} = \mathbf{0}$.

A.2. Expression of Matrix \mathbf{K}

- $\mathbf{K}(1, 1) = H_f \cos q_{f2} - (L_f - l_f) \sin q_{f2} + l_2 (\cos q_3 - \cos q_2) + l_1 (\cos q_4 - \cos q_1)$.
- $\mathbf{K}(2, 1) = H_f \cos q_{f2} - (L_f - l_f) \sin q_{f2} + l_2 (\cos q_3 - \cos q_2) + l_1 \cos q_4$.
- $\mathbf{K}(3, 1) = H_f \cos q_{f2} - (L_f - l_f) \sin q_{f2} + l_2 \cos q_3 + l_1 \cos q_4$.
- $\mathbf{K}(4, 1) = -H_f \cos q_{f2} + (L_f - l_f) \sin q_{f2} - l_2 \cos q_3 - l_1 \cos q_4$.
- $\mathbf{K}(5, 1) = -H_f \cos q_{f2} + (L_f - l_f) \sin q_{f2} - l_1 \cos q_3$.
- $\mathbf{K}(6, 1) = -H_f \cos q_{f2} + (L_f - l_f) \sin q_{f2}$.
- $\mathbf{K}(1, 2) = H_f \sin q_{f2} + (L_f - l_f) \cos q_{f2} + l_2 (\sin q_3 - \sin q_2) + l_1 (\sin q_4 - \sin q_1)$.
- $\mathbf{K}(2, 2) = H_f \sin q_{f2} + (L_f - l_f) \cos q_{f2} + l_2 (\sin q_3 - \sin q_2) + l_1 \sin q_4$.
- $\mathbf{K}(3, 2) = H_f \sin q_{f2} + (L_f - l_f) \cos q_{f2} + l_2 \sin q_3 + l_1 \sin q_4$.
- $\mathbf{K}(4, 2) = -H_f \sin q_{f2} - (L_f - l_f) \cos q_{f2} - l_2 \sin q_3 - l_1 \sin q_4$.
- $\mathbf{K}(5, 2) = -H_f \sin q_{f2} - (L_f - l_f) \cos q_{f2} - l_1 \sin q_4$.
- $\mathbf{K}(6, 2) = -H_f \sin q_{f2} - (L_f - l_f) \cos q_{f2}$.

Cite this article: M. Hobon, V. De-León-Gómez, G. Abba, Y. Aoustin and C. Chevallereau (2022). “Feasible speeds for two optimal periodic walking gaits of a planar biped robot”, *Robotica* **40**, 377–402. <https://doi.org/10.1017/S0263574721000631>